Supporting Material

Mechanistic Insights of Xenon Inhibition of NMDA Receptors from MD Simulations

Lu Tian Liu, [†] Yan Xu, [†‡§] and Pei Tang[†‡¶]*
Department of [†]Anesthesiology, [‡]Pharmacology, [§]Structural Biology, and [¶]Computational Biology, University of Pittsburgh School of Medicine, Pittsburgh, Pennsylvania 15260

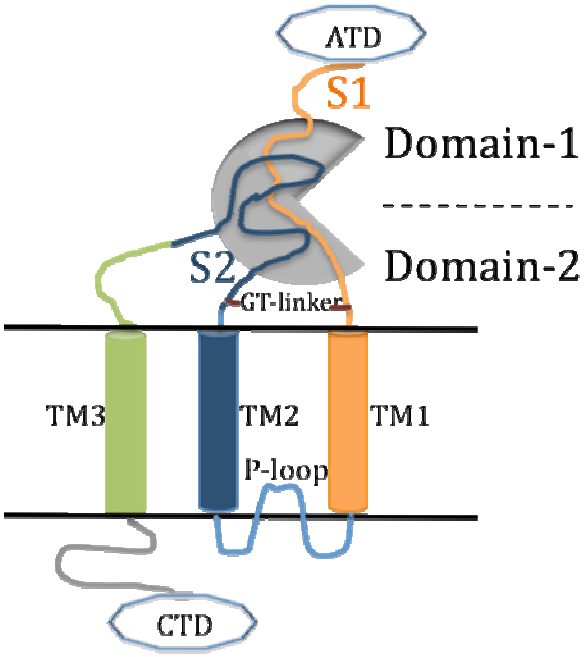

Figure S1. A carton picture showing the components for one subunit of NMDA receptor. The ligand-binding domain (LBD; highlighted in *grey half spheres*) is composed of two segments: S1 and S2 that forms two domains referred to as Domain-1 and Domain-2. The black lines highlight the boundary of lipid bilayer, within which three transmembrane domains are embedded (*TM1*, *TM2* and *TM3*). S1 is connected with ATD and TM1 and S2 is linked to TM 2 and TM3. The determined X-ray structure for the LDB has an artificial GT linker connecting S2 directly to S1, and is disconnected with ADT and TM3.

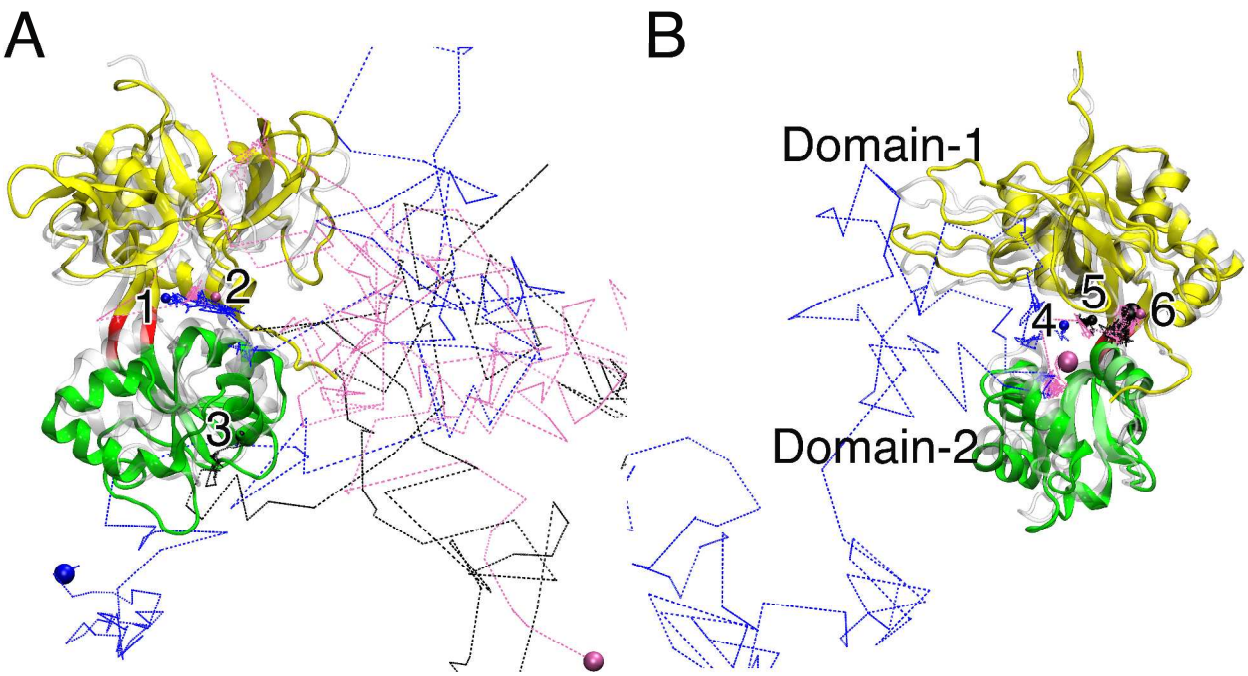

Figure S2. Xenon trajectories in the open-cleft ligand-binding domain (LBD) of NR1A (*A*) and NR1B (*B*) over the course of 20-ns simulations. The initial protein structure (PDB: 1PBQ) (*transparent and white*) is overlapped with the ending structure after 20-ns simulation (*Domain-1* in *yellow*, *Domain-2* in green, and the hinge region in *red*). Small and large spheres represent the initial and final locations of xenon, respectively. The xenon trajectories are shown in dash lines with a time step of 10ps. Four out of six xenon atoms originally in the open-cleft LBD migrated into water. Xe-5_{open} (*pink*) and Xe-6_{open} (*black*) in NR1B were relatively stable and moved only within the cleft between Domain-1 and Domain-2.

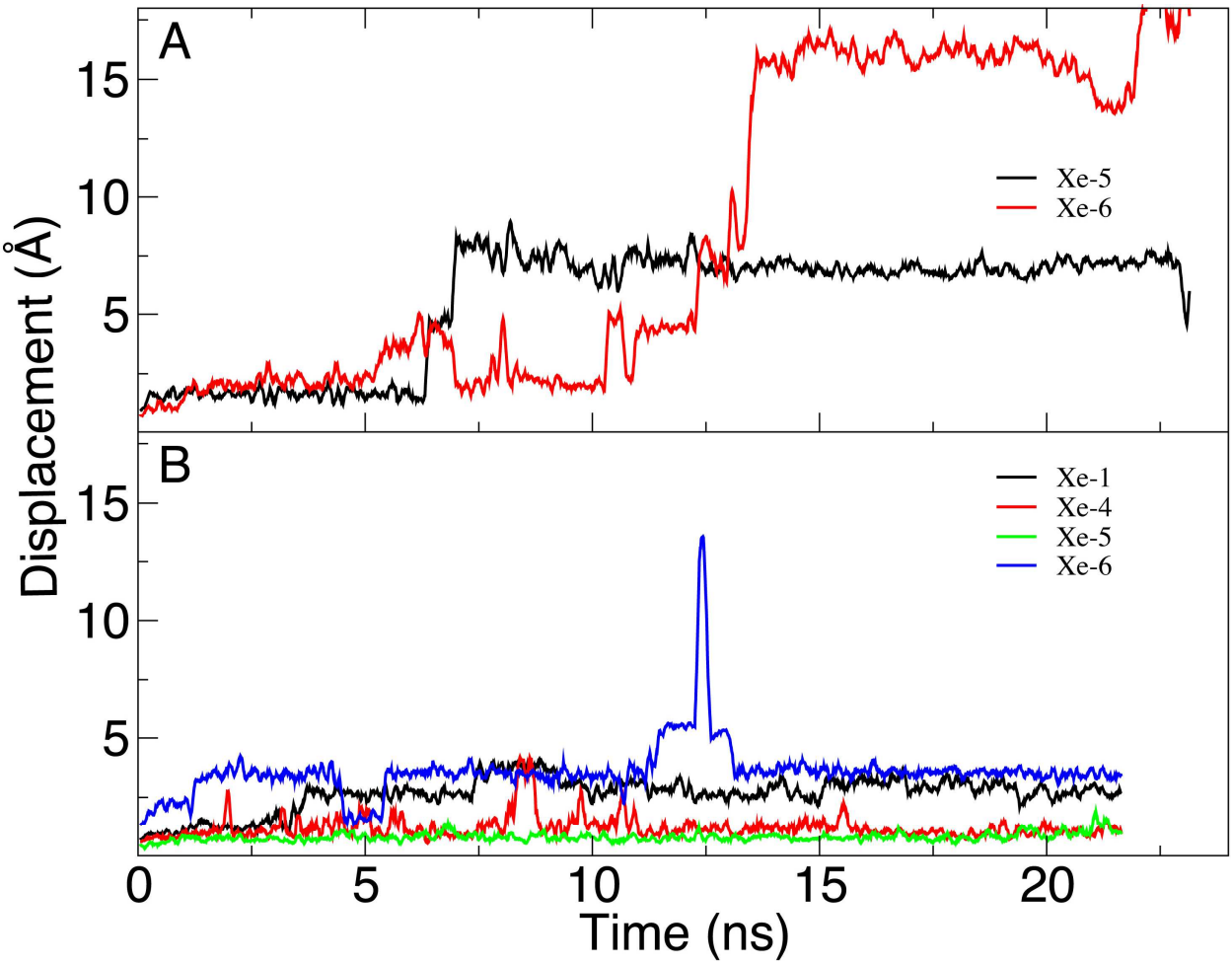

Figure S3. The displacement of relative stable xenon atoms in LBD with respect to their initial locations in the open-cleft (*A*) or closed-cleft (*B*) conformations during the 20-ns simulations. The labels are the same as those in Figure S2 and Figure 2 in the text. Overall, xenon atoms in the closed-cleft LBD had much smaller displacement than those xenon atoms in the open-cleft LBD.

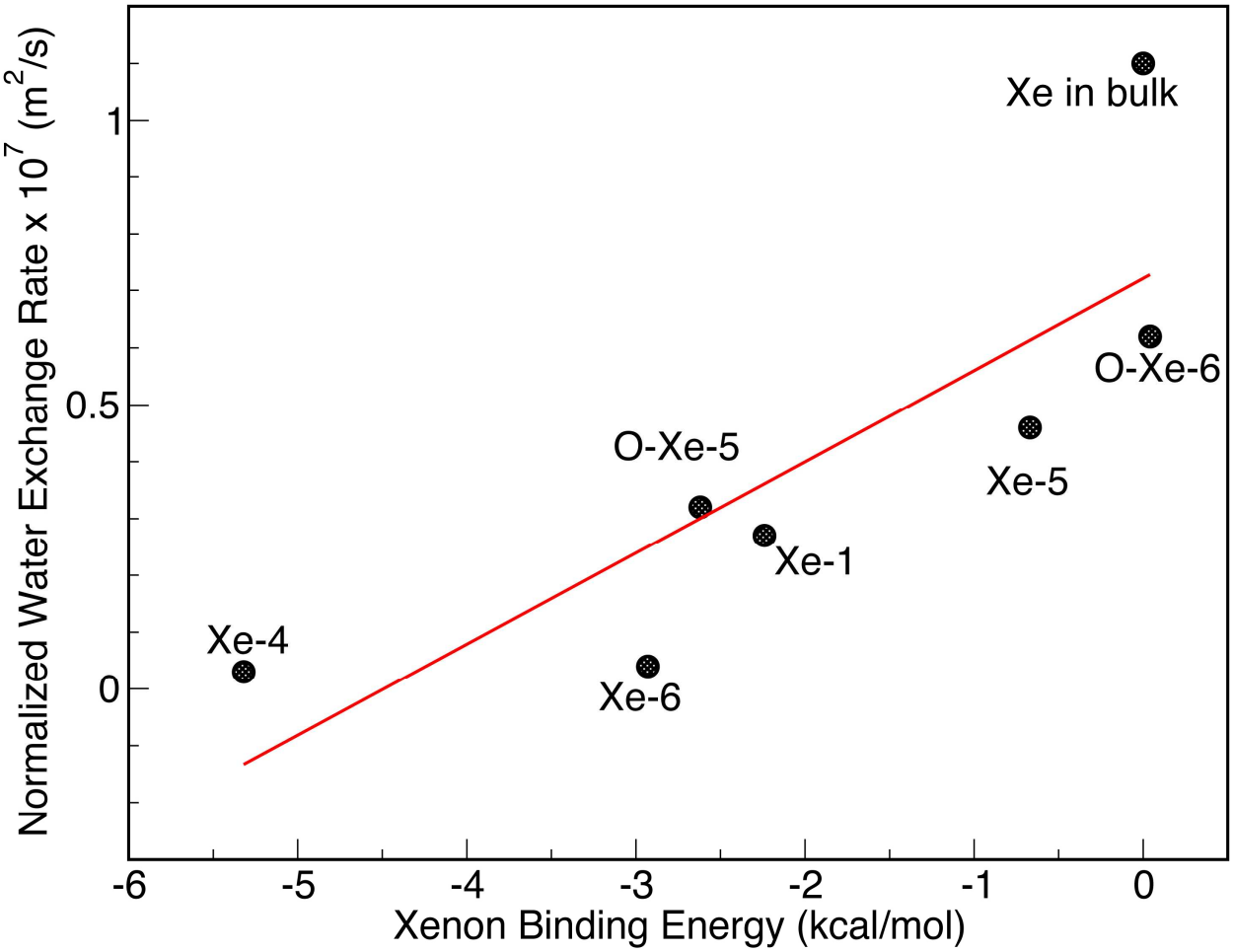

Figure S4. The association between the normalize water exchange rate around each stable xenon sites and the binding energy of individual xenon. The red line resulted from the linear regression of data. O-Xe-5 and O-Xe-6 are the two xenon atoms in the open-cleft LBD. The calculated xenon free energy in the bulk water (*1.45 kcal/mol*) agrees very well with the experimentally reported xenon solvation energy (5.6 kJ/mol) [Ben-Naim, A. *Solvation thermodynamics*. Plenum Press: New York, 1987].

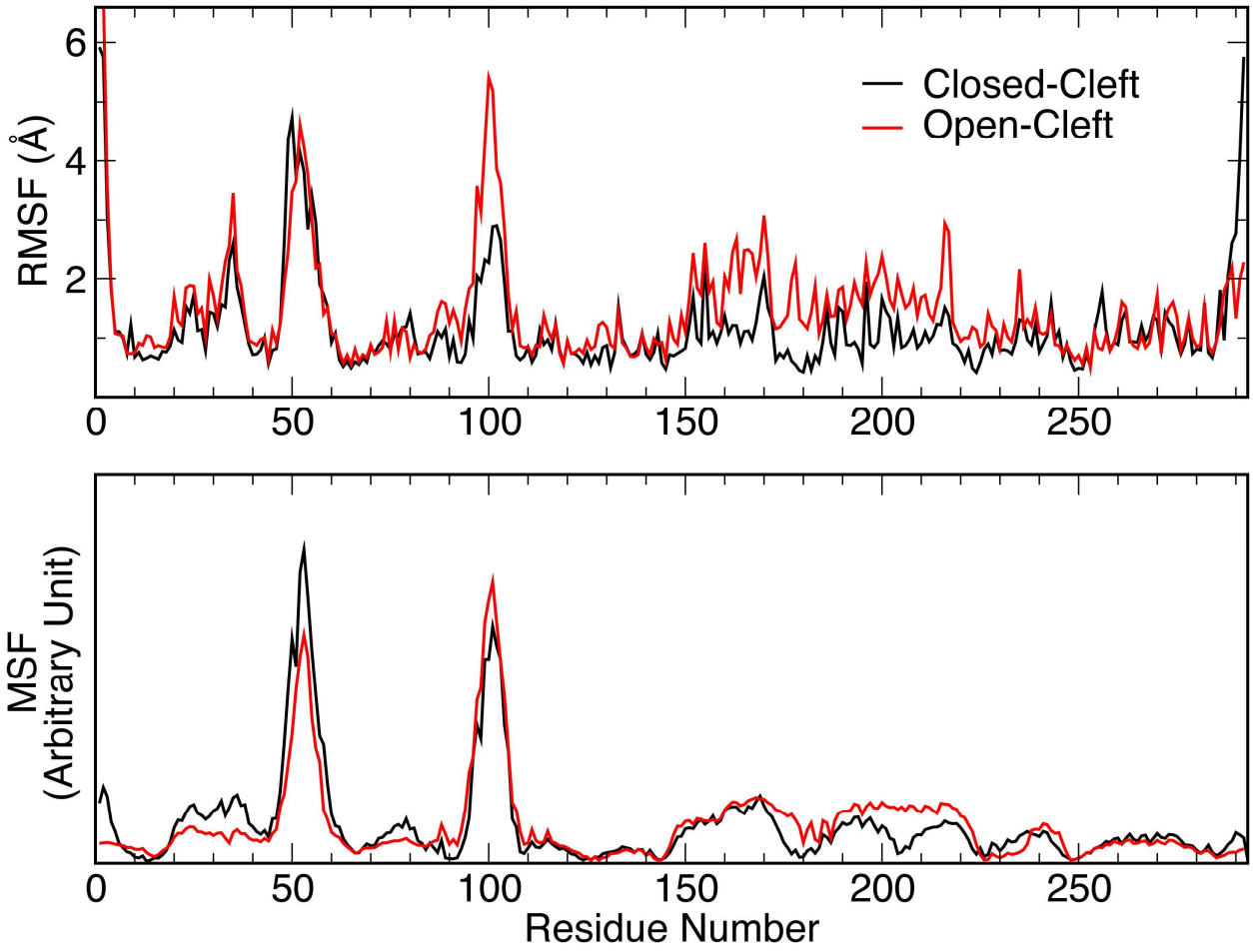

Figure S5. Top panel: the RMSFs of NR1 in the open- (*red*) and closed-cleft (*black*) conformations were obtained from the last 5 ns simulations for the control systems. Bottom panel: the MSF of Cα atoms of NR1 in the open- (*red*) and closed-cleft (*black*) conformations in the control systems, obtained from the three slowest frequency modes of GNM analysis.

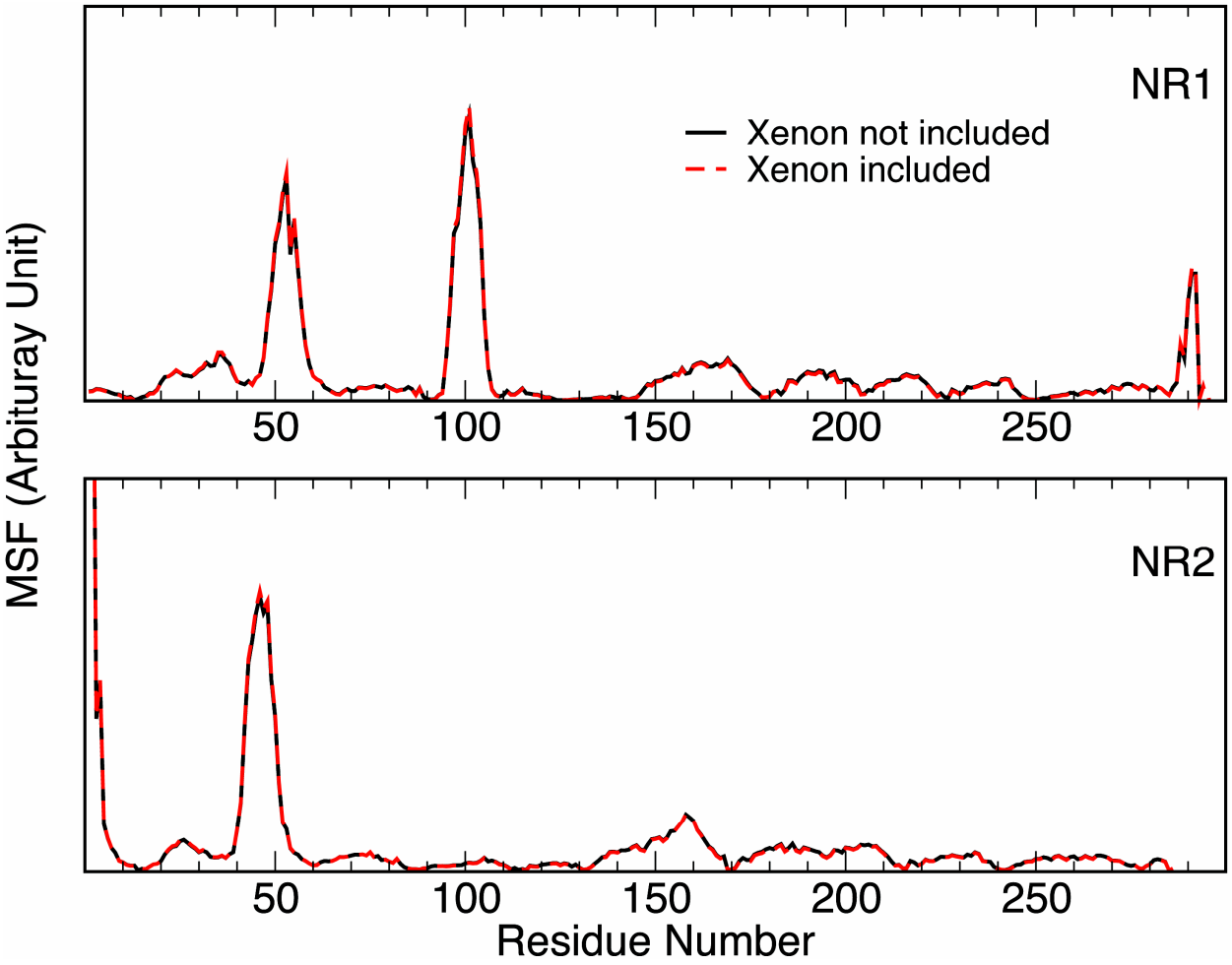

Figure S6. MSF of Cα atoms of NR1 (top panel) and NR2 (bottom panel) in closed-cleft conformation in the xenon system, obtained from the three slowest frequency modes of GNM analysis. GNM analysis showed almost identical results for calculations performed with (*red*) and without (*black*) xenon atoms included in building the contact matrix.

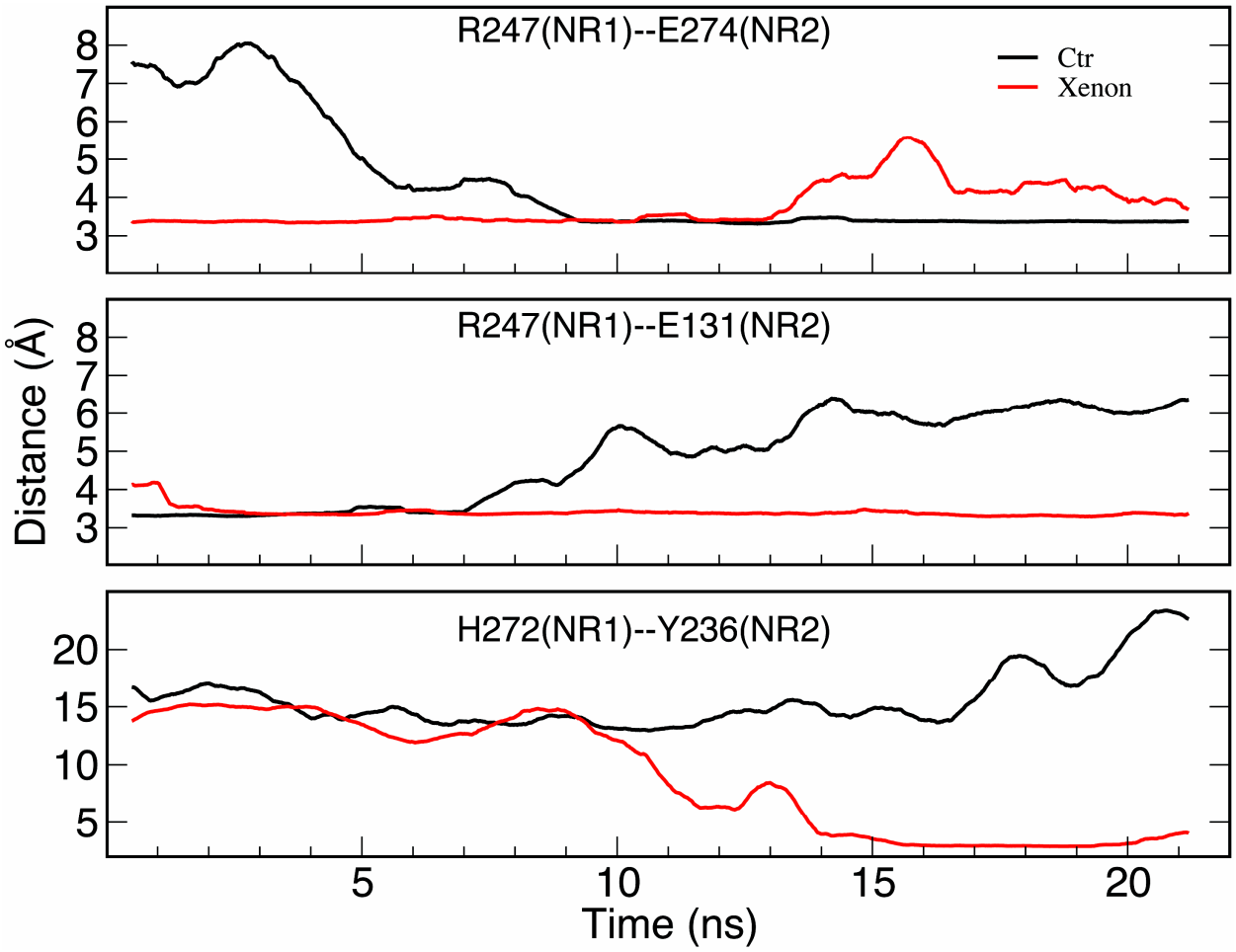

Figure S7. The distances between the pairs of residues located at the interface of NR1 and NR2 subunit during the 20-ns simulation. Changes in these distances correspond to changes in the electrostatic interaction pattern, which might account for the reduced GT-linker distance in the presence of xenon, as shown in Figure 6 in the main text.